ARTICLE

Missense Variants in *RHOBTB2* Cause a Developmental and Epileptic Encephalopathy in Humans, and Altered Levels Cause Neurological Defects in *Drosophila*

Jonas Straub,[1,20] Enrico D.H. Konrad,[1,20] Johanna Grüner,[1] Annick Toutain,[2] Levinus A. Bok,[3] Megan T. Cho,[4] Heather P. Crawford,[5] Holly Dubbs,[6] Ganka Douglas,[4] Rebekah Jobling,[7] Diana Johnson,[8] Bryan Krock,[9,10] Mohamad A. Mikati,[11] Addie Nesbitt,[9] Joost Nicolai,[12] Meredith Phillips,[5] Annapurna Poduri,[13,14] Xilma R. Ortiz-Gonzalez,[6,15] Zöe Powis,[16] Avni Santani,[9,10] Lacey Smith,[13] Alexander P.A. Stegmann,[17] Constance Stumpel,[17] Maaike Vreeburg,[17] Deciphering Developmental Disorders Study,[18] Anna Fliedner,[1] Anne Gregor,[1] Heinrich Sticht,[19] and Christiane Zweier[1,*]

Although the role of typical Rho GTPases and other Rho-linked proteins in synaptic plasticity and cognitive function and dysfunction is widely acknowledged, the role of atypical Rho GTPases (such as RHOBTB2) in neurodevelopment has barely been characterized. We have now identified *de novo* missense variants clustering in the BTB-domain-encoding region of *RHOBTB2* in ten individuals with a similar phenotype, including early-onset epilepsy, severe intellectual disability, postnatal microcephaly, and movement disorders. Three of the variants were recurrent. Upon transfection of HEK293 cells, we found that mutant RHOBTB2 was more abundant than the wild-type, most likely because of impaired degradation in the proteasome. Similarly, elevated amounts of the *Drosophila* ortholog RhoBTB *in vivo* were associated with seizure susceptibility and severe locomotor defects. Knockdown of *RhoBTB* in the *Drosophila* dendritic arborization neurons resulted in a decreased number of dendrites, thus suggesting a role of RhoBTB in dendritic development. We have established missense variants in the BTB-domain-encoding region of *RHOBTB2* as causative for a developmental and epileptic encephalopathy and have elucidated the role of atypical Rho GTPase RhoBTB in *Drosophila* neurological function and possibly dendrite development.

Introduction

Neurodevelopmental disorders (NDDs), comprising intellectual disability (ID), autism spectrum disorders (ASDs), and epileptic encephalopathies, are genetically extremely heterogeneous—more than 1,000 genes have been implicated to date (SysID database).[1] Next-generation sequencing technologies have greatly facilitated the identification and confirmation of disease-related genes. Using trio exome sequencing, several landmark studies have confirmed *de novo* variants as a major cause of NDDs in non-consanguineous populations.[2–5] Most NDD-associated genes, whose haploinsufficiency or loss of function (LoF) causes developmental disorders, have been identified by now.[6] By contrast, many disease-associated genes in which variants alter protein function still remain to be discovered, given that interpretation of missense variants is often challenging. Other than methods with limited power, such as segregation analysis or computational prediction, the currently most valuable criteria are functional studies and the identification of the same variant or a sufficient number of similar variants in individuals with overlapping phenotypes.

After the initial finding of a *de novo* missense variant in *RHOBTB2* (MIM: 607352) in an individual with early-onset epilepsy, severe ID, movement disorder, and postnatal microcephaly, we used matchmaking platforms and collaborative efforts to assemble a total of ten individuals with a similar phenotype and *de novo* missense variants in the same gene. All identified variants cluster in the BTB-domain-encoding region of *RHOBTB2*, and three of them are recurrent. We provide further evidence for their pathogenicity by showing that degradation of mutant RHOBTB2 by the proteasome is impaired *in vitro* and that

[1]Institute of Human Genetics, Friedrich-Alexander-Universität Erlangen-Nürnberg, 91054 Erlangen, Germany; [2]Service de Génétique, Centre Hospitalier Universitaire de Tours, 37044 Tours, France; [3]Department of Pediatrics, Máxima Medical Center, 5504 DB Veldhoven, the Netherlands; [4]GeneDx, Gaithersburg, MD 20877, USA; [5]Clinical and Metabolic Genetics, Cook Children's Medical Center, Fort Worth, TX 76102, USA; [6]Division of Neurology, Children's Hospital of Philadelphia, Philadelphia, PA 19104, USA; [7]Division of Clinical and Metabolic Genetics, Department of Pediatrics, The Hospital for Sick Children, University of Toronto, Toronto, ON M5G 1X8, Canada; [8]Sheffield Children's Hospital, Sheffield S10 2TH, UK; [9]Division of Genomic Diagnostics, Children's Hospital of Philadelphia, Philadelphia, PA 19104, USA; [10]Department of Pathology and Laboratory Medicine, Perelman School of Medicine, University of Pennsylvania, Philadelphia, PA 19104, USA; [11]Division of Pediatric Neurology, Duke University Medical Center, Durham, NC 27710, USA; [12]Department of Neurology, Maastricht University Medical Center, 6202 AZ Maastricht, the Netherlands; [13]Epilepsy Genetics Program, Department of Neurology, Boston Children's Hospital, Boston, MA 02115, USA; [14]Department of Neurology, Harvard Medical School, Boston, MA 02115, USA; [15]Perelman School of Medicine, University of Pennsylvania, Philadelphia, PA 19104, USA; [16]Ambry Genetics, Aliso Viejo, CA 92656, USA; [17]Department of Clinical Genetics and School for Oncology & Developmental Biology, Maastricht University Medical Center, 6202 AZ Maastricht, the Netherlands; [18]Wellcome Trust Sanger Institute, Wellcome Trust Genome Campus, Hinxton, Cambridge CB10 1SA, UK; [19]Institute of Biochemistry, Emil-Fischer Center, Friedrich-Alexander-Universität Erlangen-Nürnberg, 91054 Erlangen, Germany
[20]These authors contributed equally to this work
*Correspondence: christiane.zweier@uk-erlangen.de
https://doi.org/10.1016/j.ajhg.2017.11.008.

altered amounts of RhoBTB in the nervous system of *Drosophila melanogaster* result in seizure susceptibility, neurological defects, and disturbed dendrite development.

Material and Methods

Affected Individuals

Trio exome sequencing on an Illumina HiSeq 2500 platform in individual 1 was performed to reveal genetic causes of phenotypes similar to Pitt-Hopkins syndrome. After identification of a *de novo* variant in *RHOBTB2*, we contacted colleagues and searched DECIPHER[7] and GeneMatcher[8] for further individuals with variants in this gene. The resulting variants had been revealed in diagnostic or research settings by trio exome sequencing in various centers worldwide. *De novo* occurrence was confirmed in all individuals. Informed consent was obtained from parents or guardians of all affected individuals. If done in a research setting, the studies were approved by the ethic committees of the respective universities or centers. *In silico* prediction was performed with online programs SIFT,[9] PolyPhen-2,[10] MutationTaster,[11] and M-CAP.[12] Mutational screening of all coding exons of *RHOBTB2* (conditions and primer sequences are available on request) was performed in approximately 275 individuals with Pitt-Hopkins-like ID but without a pathogenic variant in *TCF4* (MIM: 602272) and in 96 further individuals with severe ID.

Structural Modeling

Modeling of the BTB domains was performed with the LOMETS server.[13] For the first and second BTB domain, the template structures 1R28[14] and 1I3N,[15] respectively, were used. Variants were modeled with Swiss-PdbViewer,[16] and RasMol[17] was used for structure analysis and visualization.

Protein Analysis

Human *CUL3* (MIM: 603136) and *RHOBTB2* were amplified from cDNA derived from RNA from whole blood and adult lung, respectively (Human Multiple Tissue cDNA Panel I, Clonetech) (primer sequences were 5′-CCCGCCTTAAATGTGACACC-3′ [forward] and 5′-TGATGTTGGAAACTCTCAAAGGG-3′ [reverse] for *CUL3* and 5′-CAGTAAACAAGAATATGCACGCG-3′ [forward] and 5′-CTGTAAGGTGGATGGGGTGATG-3′ [reverse] for *RHOBTB2*), and cloned into a pCR 2.1-TOPO vector (Thermo Fisher Scientific). Sanger sequencing of clones confirmed integrity, apart from a silent single-base-pair exchange (c.930T>C) in the *RHOBTB2* construct. After site-directed mutagenesis using a modified version of the QuikChange Site-Directed Mutagenesis protocol (StrataGene), wild-type and mutant *RHOBTB2* cDNAs were transferred into a pcDNA3.1 expression vector (Thermo Fisher Scientific) and a His-cMyc-tagged version of the pcDNA3.1 vector, respectively, and *CUL3* was cloned into a HA-tagged CMV expression vector.

For co-immunoprecipitation, HEK293 cells were grown in 6-well plates and co-transfected with 1 μg of His-cMyc-tagged wild-type or mutant *RHOBTB2* and with 1 μg of HA-tagged *CUL3* with Lipofectamine 2000 and PLUS reagent (Thermo Fisher Scientific). The empty pcDNA3.1-His-cMyc plasmid was transfected as a negative control. 24 hr after transfection, new medium containing 25 μM of MG-132 proteasome inhibitor (Sigma-Aldrich) was added. After 4 hr, cells were trypsinized, washed three times with 1× PBS, and lysed (buffer: 100 mM TRIS-HCl [pH 8], 150 mM NaCl, 1 mM EDTA, and 1% Triton X-100). Protein concentrations were measured with a Qubit 1.0 fluorometer (Thermo Fisher Scientific), and 1.5 mg of protein per sample was adjusted to 300 μL with 1× TBS. Immunoprecipitation was performed with 20 μL Protein A Mag Sepharose bead suspension (GE Healthcare), which was incubated with the sample and 1.6 μg anti-cMyc antibody (Sigma-Aldrich) at 4°C overnight. As controls, lysates from cells transfected with wild-type *RHOBTB2* were incubated either with beads only or with beads and mouse IgG. Subsequently, the supernatant was removed, and beads were washed once with lysis buffer and four times with 1× TBS. Samples were eluted with 2× NuPAGE sample buffer and 10% DTT and stored at −80°C.

For overexpression analysis, HEK293 cells were transfected with 1 μg of wild-type or mutant *RHOBTB2* with or without 1 μg of the *CUL3* construct as described above. 24 hr after transfection, cells were trypsinized, washed three times with cold 1× PBS, and lysed (buffer: 100 mM TRIS, 150 mM NaCl, and 1% Triton X-100 [pH 7.5]). Lysates were frozen at −80°C. MG-132 was added to a final concentration of 5 μM for 16 hr. To exclude major differences in transfection efficiency and to exclude higher protein amounts based on mRNA overexpression, we performed quantitative PCR on RNA from cells taken from the same wells as the protein lysate (Figure S1).

For western blotting, the NuPAGE 4%–12% Bis-Tris Gel System (Thermo Fisher Scientific) was used. After blocking, incubation with primary antibodies was performed overnight at 4°C. Antibodies against RHOBTB2 (SAB1407189) and CUL3 (C0871) were obtained from Sigma-Aldrich and used in 1:400 and 1:2,000 dilution, respectively. Tagged proteins were detected with antibodies against cMyc (M4439) and HA (H6908) (Sigma-Aldrich). Alpha-tubulin or beta-actin (Abcam) was used as a loading control. To reduce background, we cut and incubated blot membranes separately with either an antibody against RHOBTB2 or the loading control. Secondary, horseradish-peroxidase-conjugated antibodies (anti-mouse [Abnova] and anti-rabbit [Bio-Rad]) were applied for 2 hr at room temperature. Blots were scanned on a C-DiGit blot scanner (LI-COR), and images were exported as TIFFs for analysis in ImageJ.[18] For quantification, rectangles were drawn around each western blot lane, and density was measured. The areas under the peak corresponding to RHOBTB2 were measured and normalized to those of the corresponding loading control.

Fly Lines and Conditions

Flies were raised on standard food containing cornmeal, sugar, and yeast. Knockdown or overexpression was achieved with the UAS/GAL4 system.[19] Given that high breeding temperatures result in stronger knockdown effects,[20] crosses were carried out at 28°C to induce knockdown and at 25°C to induce overexpression. Driver lines were obtained from the Bloomington Stock Center or assembled in house and by colleagues (*Act5C*-GAL4/*CyO* [ubiquitous expression]; *D42*-GAL4 [expressed in motoneurons], BL#8816; *OK6*-GAL4 [expressed in motoneurons, type I terminals], BL#64199; *DJ757*-GAL4 [expressed in muscle], BL#8184; *repo*-GAL4 [expressed in glia], BL#7415; UAS-*Dcr*-2;477-GAL4,UAS-mCD8::GFP;ppk-GAL4/Tm3sb [expressed in class IV dendritic arborization (da) neurons];[21] *elav*-GAL4;UAS-*Dcr*-2 [pan-neuronal expression]; *elav*-GAL4/*Cyo* [pan-neuronal expression]; *elav*-GAL4;*elav*-GAL4 [pan-neuronal expression]; UAS-*Dcr*-2; *elav*-GAL4 [pan-neuronal expression]; and UAS-*Dcr*-2;*247*-GAL4 [expressed in mushroom body]). RNAi lines were obtained from the Transgenic RNAi Project[22] (TRiP) (BL#32416

and BL#36303 [control]) and from the Vienna *Drosophila* Research Center (VDRC) (100815/KK and 60100 [control]; 330130 and 60200 [control]).[23] We confirmed reduced *RhoBTB* expression to ca. 40% for ubiquitous knockdown by using the BL#32416 TRiP line and to 50% by using the 100815 VDRC line (referred to as RNAi_RhoBTB_1 and RNAi_RhoBTB_2, respectively; Figures S2B and S2C). Because VDRC line 100815 was revealed to carry an additional insertion that can cause dominant phenotypic effects such as wing anomalies and lethality,[24] we used it only to confirm phenotypes observed with the TRiP line. VDRC line 330130 (referred to as RNAi_RhoBTB_3; Figure S2D) was shown to not induce knockdown and was therefore excluded from experiments. An available mutant ($RhoBTB^{MB07044}$, BL#26065) was shown to be hypomorphic with a knockdown to only 50% (Figure S3A). Because it was additionally white eyed and lacked an isogenic control, we used it only to test bang sensitivity.

For the generation of UAS-driven overexpression lines, *RhoBTB* was PCR amplified from whole fly cDNA (primer sequences 5′-GC TGGTTCTGCTATTTGTGC-3′ [forward] and 5′- TATCTCCCCGA CCACTCTAAATC-3′ [reverse]) and cloned into a pUAST fly expression vector.[19] After sequence verification of the clone, BestGene used the construct to create transgenic flies. On the basis of quantitative real-time PCR after ubiquitous overexpression, we selected two lines with 60- or 30-fold overexpression (referred to as UAS-*RhoBTB*_1: UAS-*RhoBTB*_1; +/+ or UAS-*RhoBTB*_2: +/+; UAS-*RhoBTB*_2, respectively; Figure S2A).

Bang Sensitivity

Bang sensitivity is characterized by paralysis and hyperactivity after a mechanical shock and can be induced by vortexing at maximal strength for 10 s.[25] *RhoBTB* lines and the corresponding genetic background control lines were crossed to the *elav*-GAL4;UAS-*Dcr*-2 (RNAi-induced knockdown) or *elav*-GAL4/*Cyo* (overexpression) (both pan-neuronal) driver lines. A minimum of 50 flies per genotype and matching controls were collected 0–48 hr after eclosion under CO_2 anesthesia in groups of ten (with a balanced male/female ratio) and kept in normal food vials for 24 hr. After transferal to testing vials and an adjustment time of 1 min, flies were vortexed for 10 s. The number of flies displaying paralysis or spasms 5 s after vortexing was assessed.

Negative Geotaxis

Negative geotaxis experiments were carried out as described by Palladino et al.[26] with some modifications. *RhoBTB* overexpression and RNAi lines and the corresponding genetic background control lines were crossed to *elav*-GAL4/*Cyo* (pan-neuronal), *OK6*-GAL4 and *D42*-GAL4 (motoneuron), *DJ757*-GAL4 (muscle), and *repo*-GAL4 (glia) driver lines. A minimum of 300 flies per genotype and matching controls were collected and prepared for trial as described for the bang-sensitivity assay. After transferal to testing vials and an adjustment time of 1 min, flies were tapped to the bottom of the vial and videotaped for 30 s. From the tapes, time was measured until 70% of flies had climbed 8.8 cm.

Neuromuscular Junctions

Analysis of type 1b neuromuscular junctions (NMJs) of muscle 4 was performed as described previously.[27] *RhoBTB* overexpression and RNAi lines and corresponding genetic background control lines were crossed to *elav*-GAL4;*elav*-GAL4 or UAS-*Dcr*-2;*elav*-GAL4 (pan-neuronal) and *OK6*-GAL4 and *D42*-GAL4 (motoneuron) driver lines. In brief, male L3 larvae were dissected, fixated in 4% paraformaldehyde, and stained with nc82 and anti-dlg antibodies (Developmental Studies Hybridoma Bank). Secondary antibodies used were Alexa-488-labeled anti-mouse antibody and the Zenon Alexa Fluor 546 Mouse IgG1 Labeling Kit (Life Technologies). Images were taken with a Zeiss Axio Imager Z2 microscope with 10× and 63× objectives, and NMJ pictures were subsequently stacked and analyzed in ImageJ. Synaptic area and length and numbers of synaptic branches, boutons, and active zones were determined under genotype-blind conditions. For each genotype, at least 11 synapses from four to nine different animals were analyzed.

Dendritic Arborization Neurons

RhoBTB overexpression and RNAi lines and the corresponding genetic background control lines were crossed to the UAS-*Dcr*-2;477-GAL4,UAS-mCD8::GFP;ppk-GAL4/Tm3sb (active in class IV da neurons) driver line. Male L3 larvae were dissected from the ventral side and fixated in 4% paraformaldehyde. Staining of solitary type IV multidendritic sensory neurons in the larval body wall was performed with rat antibody against mouse CD8A[28] (Thermo Fisher Scientific) and Alexa-488-labeled anti-rat secondary antibodies. The number and length of dendritic branches were determined in ten neurons from three to five different animals per genotype with NeuronJ[29] using 2D image projections of Z stacks acquired on a Zeiss (LSM 800) confocal microscope using a 20× objective.

Statistical Analysis

Data from neuron experiments on bang sensitivity, negative geotaxis, NMJs, and da were averaged, and testing for statistical significance was performed with a two-tailed Wilcoxon rank-sum test.

Results

Clinical Phenotype

Epilepsy manifested in all of the individuals reported here within the first 3 years of life (between the first week and ninth month in nine of ten individuals). Seizure types were variable and included focal dyscognitive and generalized tonic-clonic seizures, as well as febrile seizures in the mildest affected individual; five individuals experienced status epilepticus. Apart from individuals 3 and 4, response to antiepileptic treatment was reported to be good, and febrile seizures in individual 10 ceased spontaneously. Neurodevelopment was severely impaired in all individuals through a lack of or delayed mobility and speech abilities. Developmental stagnation was reported in one individual and regression was reported in five, correlating with the onset or worsening of epilepsy. Cognitive impairment was mildest in individuals 8 and 10, who showed a relatively late onset of epilepsy and had only febrile seizures, respectively. Hemiparesis was observed in four individuals (after seizures in three of them). In this context, brain imaging in individual 5 revealed acute diffusion anomalies and subsequent atrophy and infarction anomalies. MRI in individual 4 also revealed progressive atrophy, and MRI in individual 8 showed hemispheric swelling (diffusion negative) within a week of onset of

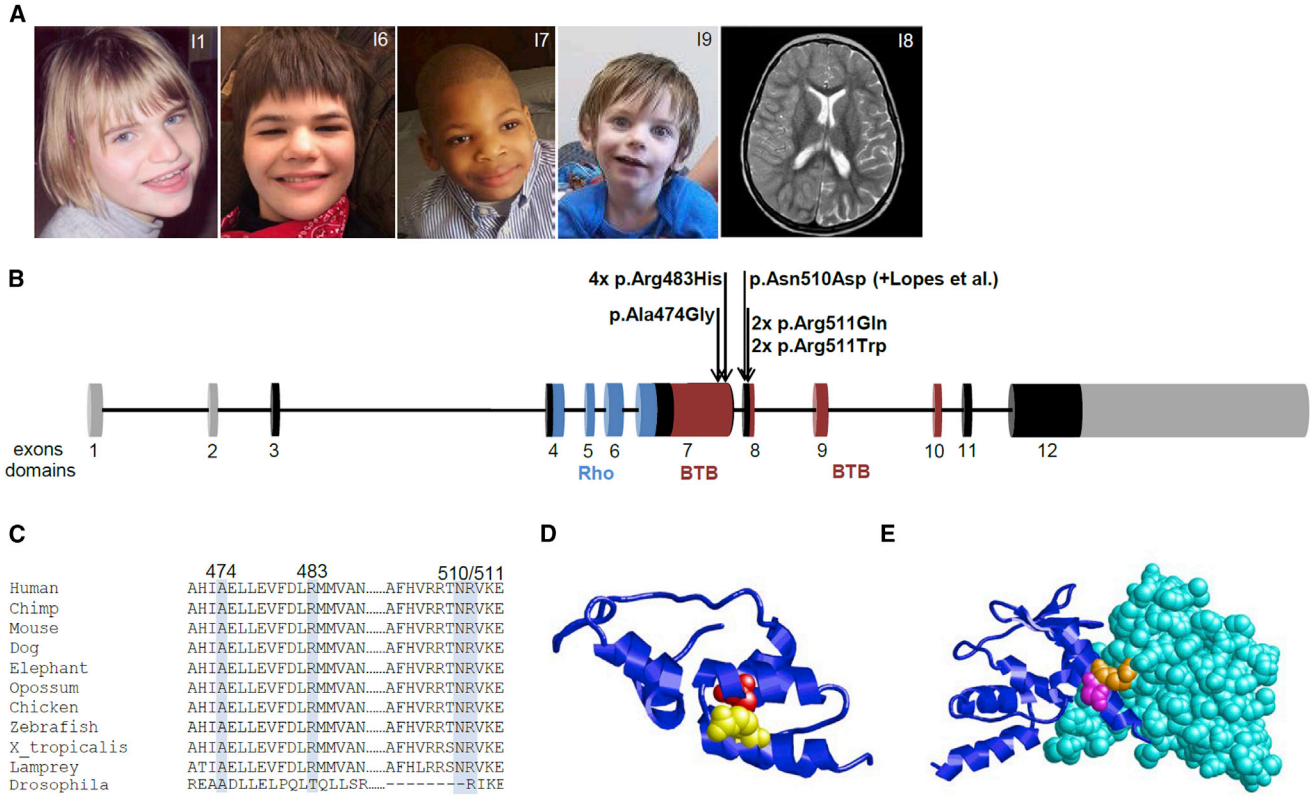

Figure 1. Mutations in *RHOBTB2*

(A) Clinical pictures of individuals with pathogenic variants in *RHOBTB2* show minor and unspecific dysmorphic aspects, and an MRI axial T2 image corresponding to individual 8 demonstrates right hemispheric edema in the setting of acute left hemiparesis.

(B) Schematic drawing of *RHOBTB2* (longest isoform: GenBank: NM_001160036.1) includes non-coding (gray) and coding (black) exons and encoded domains (colored) according to SMART.[30] The variants identified here and one published variant[31] cluster within the BTB-domain-encoding region.

(C) Conservation of the affected amino acids according to the UCSC Browser is depicted with Clustal Omega.

(D) Model of the first BTB domain (blue ribbon presentation). Residues Ala474 and Arg483 are highlighted in red and yellow, respectively.

(E) Model of the second BTB domain in the homodimeric state. The subunits are shown as blue ribbon and cyan spaced-filled presentations. Residues Arg511 and Asn510 are highlighted in orange and magenta, respectively.

left hemiparesis (Figure 1A). Earlier MRI and MRI in most of the other individuals showed normal results or no specific findings, such as delayed myelination or enlarged ventricles and a thin corpus callosum. Truncal hypotonia was noted in nine individuals, and five showed additional limb hypertonia, even requiring Botox injections in individual 9. Dystonic, paroxysmal, or chorea-like movements were also observed in all but individuals 4 and 10. Although birth measurements appeared to be normal, postnatal, progressive microcephaly was common, and postnatal growth retardation occurred in five individuals. In most of the individuals, minor but unspecific dysmorphic aspects were noted (Figure 1A). Additional clinical details are presented in Table 1.

Mutational Spectrum

In ten individuals, we identified five different *de novo* missense variants in *RHOBTB2*. The c.1448G>A (p.Arg483His) variant was found in four individuals. Arginine at position 511 was recurrently affected by two different missense variants in four individuals. c.1421C>G (p.Ala474Gly) was identified in a single individual (Table 1). Also, c.1528A>G (p.Asn510Asp) was identified in one individual but was reported in another individual with a Rett-syndrome-like phenotype.[31] Variants were identified in several centers worldwide and assembled through contact with colleagues and searches in DECIPHER[7] and GeneMatcher.[8] In-house screening of *RHOBTB2* in approximately 370 individuals with severe ID did not reveal further pathogenic variants.

According to exome sequencing data from the Exome Aggregation Consortium (ExAC) Browser,[32] *RHOBTB2* is tolerant of LoF (probability of LoF intolerance [pLI] = 0.51) and carries more copy-number variants (CNVs) (Z score = 0.49) but fewer missense variants than expected (Z score = 3.29). DECIPHER contains no small CNVs affecting only *RHOBTB2*, thus not allowing gene-specific interpretation.

None of the identified variants in our study is present in the ExAC Browser or GnoMAD, and all are predicted to (probably) be pathogenic by several prediction programs (Table S1). All variants cluster in the region of the two

Table 1. Clinical Details of Individuals with *De Novo* Missense Variants in *RHOBTB2*

	Individual 1	Individual 2	Individual 3	Individual 4	Individual 5	Individual 6	Individual 7	Individual 8	Individual 9	Individual 10
Gender	female	male	female	female	female	female	male	male	male	female
Age	8 years, 4 months	3.5 years	8 years	11 years	14 years	17 years	7 years	3 years	23 months	11.5 years
De novo variant (GenBank: NM_001160036.1)	c.1448G>A (p.Arg483His)	c.1448G>A (p.Arg483His)	c.1448G>A (p.Arg483His)	c.1448G>A (p.Arg483His)	c.1532G>A (p.Arg511Gln)	c.1532G>A (p.Arg511Gln)	c.1531C>T (p.Arg511Trp)	c.1531C>T (p.Arg511Trp)	c.1528A>G (p.Asn510Asp)	c.1421C>G (p.Ala474Gly)
Birth weight (SD)	2,945 g (−1.37)	3,570 g (0.45)	NA	3,487 g (0.03)	3,780 g (0.35)	3,459 g (0.09)	2,410 g (−0.73)	3,200 g (−0.96)	2,720 g (−0.32)	3,770 g (−0.03)
Birth length (SD)	49 cm (−1.04)	54.8 cm at 1 month (−0.46)	NA	NA	51 cm (−0.13)	53 cm (1.13)	NA	51 cm (−0.65)	49.5 cm (−0.81)	55.5 cm (1.57)
Birth OFC (SD)	33.5 cm (−1.25)	37.6 cm at 1 month (−0.59)	NA	NA	37 cm at 6 weeks (−0.3)	NA	36.3 cm at 3 weeks (0)	NA	34 cm (0.13)	38 cm (1.76)
Height (SD)	107 cm at 6 years (−1.59)	90 cm at 2.5 years (−2.29)	NA (−2.2)	116.6 cm at 8 years (−2.30)	138 cm (−3.42)	157 cm (−0.93)	117 cm (−0.23)	88 cm (−2.65)	81.8 cm (−1,73)	122 cm at 6.25 years (0.89)
Weight (SD)	17 kg at 6 years (−1.34)	11.9 kg at 2.5 years (−0.91)	NA (−0.45)	19.7 kg at 8 years (−2.16)	25 kg (−5.4)	54.4 kg (−0.13)	23.2 kg (0.45)	15.3 kg (−0.2)	7.92 kg (−3.63)	20.7 kg at 6 years (−0.13)
OFC (SD)	47 cm (−3.08)	43.8 cm at 8 months (−0.49)	46.9 cm at 7 years, 7 months (−3.9)	48 cm (8 years) (−2.83)	49 cm (−3.8)	52 cm (−1.98)	49.5 cm (−1.88)	47 cm (−3.7)	43.5 cm (−4.49)	49.7 cm at 6.25 years (−1.19)
Walking (age)	no	no (2.5 years)	no	no	with support	short distances	a few steps (5 years)	yes (3 years)	no	yes (1.5 years)
Speech abilities	few short words	non-verbal	non-verbal	non-verbal	non-verbal	non-verbal	non-verbal	few short words	non-verbal	rare two-word combination
Comprehension	severely limited	limited	turns to voice only	limited	none	severely limited	severely limited	good	very limited	good
Regression (age)	no	no	yes (6 months)	yes, after seizures	yes	possibly (4 months)	no	yes (3 years)	stagnation (4 months)	no
DD or ID	severe	severe	profound	severe	severe (IQ < 30)	severe	severe	moderate	severe	severe
Seizure onset (type)	2 months	4 days (generalized)	6 months (SE)	10 weeks (focal, sec. general.; later SE)	4 weeks (2× SE)	4 months	4 months (complex partial, GTC)	3 years (focal status)	9 months (SE)	5.5 months (febrile)
Antiepileptic treatment	carbamazepine from 3.5 years	neonatally phenobarbital, then carbamazepine	divalproex sodium, topiramate, zonisamide ketogenic diet, lacosamide, clobazam, phenobarbital, levetiracetam	phenobarbital, levetiracetam, clonazepam, memantine	valproic acid, pyridoxine	carbamazepine (previously lamotrigine, topiramate, phenobarbital)	levetiracetam	levetiracetam	levetiracetam	none

(*Continued on next page*)

Table 1. ***Continued***

	Individual 1	Individual 2	Individual 3	Individual 4	Individual 5	Individual 6	Individual 7	Individual 8	Individual 9	Individual 10
Response to treatment	yes; no seizures from the age of >4 years	good for seizures, partial for dystonic attacks	drug resistance	no seizures from the age of 4 years, then refractory including SE	yes; response to pyridoxine (two seizures per year)	yes	yes	yes	yes; no seizures from the age of >9 months	NA; no febrile seizures from the age of >6 years
MRI anomalies	no	delayed myelination	enlarged ventricles, prominent cortical sulci, thin CC	thin CC, cerebellar hypoplasia, prominent opercula, later cortical atrophy	secondarily acute diffusion and white-matter abnormalities, atrophy	no	no	right hemispheric swelling after left hemiplegia and focal seizures	no	no
Hypotonia	truncal	yes	yes	truncal	yes	yes	truncal	axial	truncal	no
Hypertonia	lower limbs	NA	NA	limbs	NA	no	limbs	mild left spastic hemiparesis	lower limbs	no
Movement disorders	paroxysmal	choreatic, dystonic, paroxysmal dyskinetic attacks	dystonic	no	yes	dystonic	paroxysmal, dystonic-athetoid attacks	paroxysmal dystonic attacks	chorea-like, limbs	no
Stereotypies	no	no	no	hand movements	no	repetitive behaviors	no	no	hands in mouth	no
Behavioral anomalies	limited interaction, easy smiling and laughing	no	no	no	pleasant behavior	noise sensitivity, self-harm (exacerbated by anxiety)	yes	no	intense stare, uncontrollable laughter, bruxism, pleasant behavior	autistic, biting, head banging
Facial dysmorphism	Pitt-Hopkins-like	low nasal bridge, epicanthal folds	hirsute long eyelashes, micrognathia, large pinnae	sparse eyebrows, deep-set eyes, depressed nasal root, slightly low insertion of columella	full lower lip, flat maxillae	deep-set eyes, epicanthal folds, low anterior hairline, thick arched eyebrows, broad nasal tip	dolichocephaly, wide-spaced teeth	slightly smooth philtrum	large ears, thin upper lip, slightly upturned nose	long philtrum
Other anomalies	6–7 months: transient strabismus, mild constipation	no	3 years: left hemiplegia after SE	hemiparesis after SE	14 years: acute onset of hemiparesis during febrile short-lasting seizure	no	hyperreflexia, mild oculomotor apraxia, insomnia, constipation	left hemiplegia, bilateral fifth-finger clinodactyly	no	no

(*Continued on next page*)

Table 1. *Continued*

	Individual 1	Individual 2	Individual 3	Individual 4	Individual 5	Individual 6	Individual 7	Individual 8	Individual 9	Individual 10
Further, previous (genetic) testing with normal or unclear results	karyotype, array CGH, SNRPN, ARX, TCF4, MECP2, MEF2C	HR-array, POLG, SCN1A, metabolic screening, NGS panel congenital encephalopathy	mitochondrial analysis (muscle)	NA	metabolic screening, UBE3A, MECP2, SNRPN, mito DNA panel, SNP array (dup22q11.2)	metabolic screening, microarray, MECP2, CDKL5, FOXG1, SNRPN, epilepsy panel	microarray, FRM1, SNRPN, MECP2, FOXG1 (paternal 3 bp insertion)	metabolic screening, mild elevated CK, SNP array (746 kb deletion in 1p21.3)	metabolic screening, karyotype, microarray	metabolic screening, karyotype, array CGH, SNRPN, FMR1
Other WES result	no	no	no	NA	no	no	no	paternally inherited VUS in CACNA1A (p.Arg1235His [c.3704G>A])	no	no

Abbreviations are as follows: abn., abnormalities; CC, corpus callosum; CGH, comparative genomic hybridization; CK, creatine kinase; comb., combination; DD, developmental delay; GTC, generalized tonic clonic; ID, intellectual disability; mito, mitochondrial; NA, not available or not applicable; OFC, occipitofrontal head circumference; SE, status epilepticus; sec. general., secondary generalization; VUS, variant of unknown significance; and WES, whole-exome sequencing.

BTB domains (Figure 1B) and affect highly conserved amino acids (Figure 1C). Molecular modeling of the first BTB domain revealed that Ala474 and Arg483 are located in immediate spatial vicinity, and both form stabilizing interactions within the domain (Figure 1D). Asn510 and Arg511 are located on a surface patch of the second BTB domain, which is involved in BTB dimer formation (Figure 1E). Molecular modeling suggests that the p.Ala474Gly and p.Arg483His variants cause a destabilization of the first BTB domain, whereas variants at positions 510 and 511 hamper dimer formation of the second BTB domain (Figures S4 and S5).

RHOBTB2 Variants Result in Increased Protein Abundance

On the basis of reports of interaction between RHOBTB2 and CUL3,[33,34] we performed co-immunoprecipitation to investigate whether the identified variants in RHOBTB2 would impair binding to CUL3. We did not observe differential binding between mutant and wild-type RHOBTB2 (Figure 2A). However, when overexpressing *RHOBTB2* in HEK293 cells, we observed that mutant protein was more abundant than wild-type RHOBTB2 after 24 hr (Figure 2B). We observed no difference when we co-transfected *CUL3* (Figure 2B) to increase its already high endogenous amounts (Figure S6), and results were confirmed and quantified in a total of four independent experiments (Figure 2C). The same result of altered protein amounts was observed with independent, His-Myc-tagged *RHOBTB2* constructs (Figure S7). Upon the addition of proteasome inhibitor, mutant and wild-type RHOBTB2 were equally abundant (Figure 2D), indicating that degradation of mutant RHOBTB2 via the proteasome is impaired. Material from affected individuals for testing for increased protein amounts was not available.

To see whether increased amounts of RHOBTB2 would result in mislocalization or abnormal protein aggregation, we performed immunofluorescence on HEK293 cells transfected with wild-type or mutant *RHOBTB2* constructs. We did not observe obvious differences in localization or distribution between mutant and wild-type RHOBTB2 (Figure S8), although mild differences cannot be excluded.

Altered Dosage of RhoBTB Leads to Neurological Phenotypes in *Drosophila*

To better characterize the role of RHOBTB2 in the nervous system and to confirm its implication in developmental and epileptic encephalopathy, we chose *Drosophila melanogaster* as a model. The *Drosophila* genome contains a single ortholog (*RhoBTB*) of the three vertebrate paralogs. Given its organization on the phylogenetic tree (HomoloGene and TreeFam), it seems to be closest to RHOBTB2.[35] To manipulate RhoBTB amounts *in vivo*, we generated inducible UAS-*RhoBTB* transgenic lines (UAS_RhoBTB_1 and UAS_RhoBTB_2)

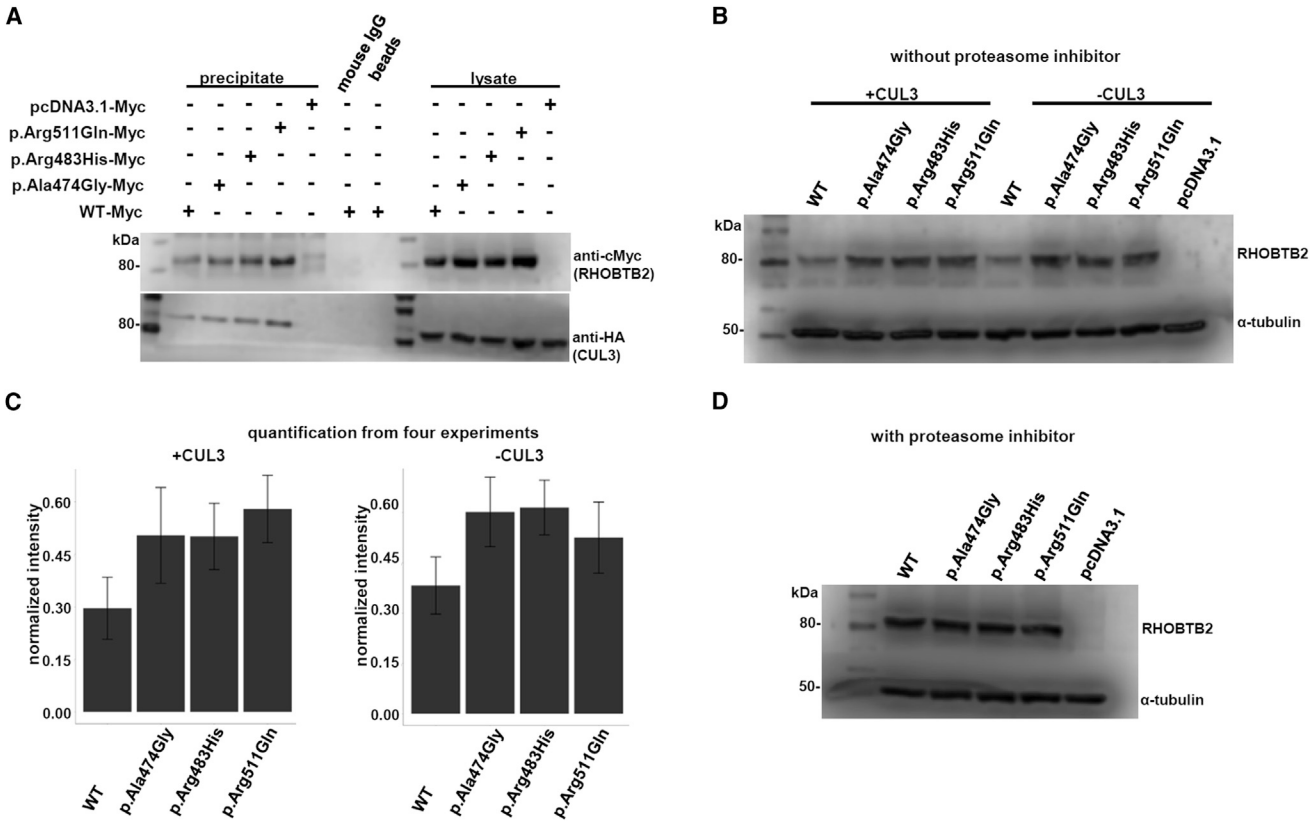

Figure 2. Co-immunoprecipitation and Analysis of Overexpressed RHOBTB2

(A) Co-immunoprecipitation of His-cMyc-tagged RHOBTB2 and HA-tagged CUL3. Precipitation was performed with an antibody against cMyc. HA-CUL3 equally co-precipitates with both mutant and wild-type RHOBTB2. Because RHOBTB2 and CUL3 are the same size, two gels for the same experiment were used and stained separately.

(B) Representative western blot after transfection of wild-type and mutant *RHOBTB2* with and without co-transfection of *CUL3*. In each condition, mutant RHOBTB2 was more abundant than the wild-type.

(C) Quantification from western blot from four independent experiments, including mean values; error bars represent the standard error of the mean (SEM).

(D) Adding proteasome inhibitor to cells transfected with wild-type or mutant RHOBTB2 and co-transfected with CUL3 resulted in equal amounts of wild-type and mutant RHOBTB2.

and obtained *RhoBTB* UAS-RNAi lines (RNAi_RhoBTB_1 and RNAi_RhoBTB_2) from the TRiP and VDRC (Material and Methods). Given the observation of increased amounts (Figure 2B) of mutant RHOBTB2, overexpression of *RhoBTB* in *Drosophila* appeared to be a good model.

Given the severe epilepsy phenotype in humans with clustering missense variants in *RHOBTB2*, we asked whether there would be similar phenotypes in flies. Seizure susceptibility in *Drosophila* can be induced by mechanical shock and is indicated by a subsequent phenotype called bang sensitivity, which is characterized by hyperactivity and paralysis.[36] We found that flies overexpressing *RhoBTB* in all neurons were bang sensitive and remained paralyzed or with spasms on the bottom of the vial after vortexing, whereas control flies recovered immediately or within a few seconds (Figures 3A and 3B and Movie S1). Compared with overexpression, pan-neuronal knockdown of *RhoBTB* resulted in no or milder bang sensitivity (Figure 3B). Similarly, we did not observe a phenotype when testing the hypomorphic mutant line (Figure S3B). These observations indicate that overexpression of *RhoBTB* particularly induces seizure susceptibility in flies.

We next investigated whether fly behavior would be compromised in other aspects of neurological functioning. We tested complex learning behavior with the courtship conditioning paradigm, but neither flies with knockdown nor flies with overexpression of *RhoBTB* in all neurons or specifically in the mushroom body, a part of the insect brain involved in learning and memory,[37] showed significantly impaired learning or short- or long-term memory (Figure S9).

In contrast, testing gross neurological and locomotor function with the negative geotaxis assay resulted in a severe locomotor phenotype. Overexpression of *RhoBTB* in several tissues (pan-neuronal, motoneurons, muscle, and glia) resulted in marked locomotor impairment, whereas RNAi-mediated knockdown caused no significant differences from the respective controls, except for pan-neuronal knockdown (Figures 3C–3E and Figure S10).

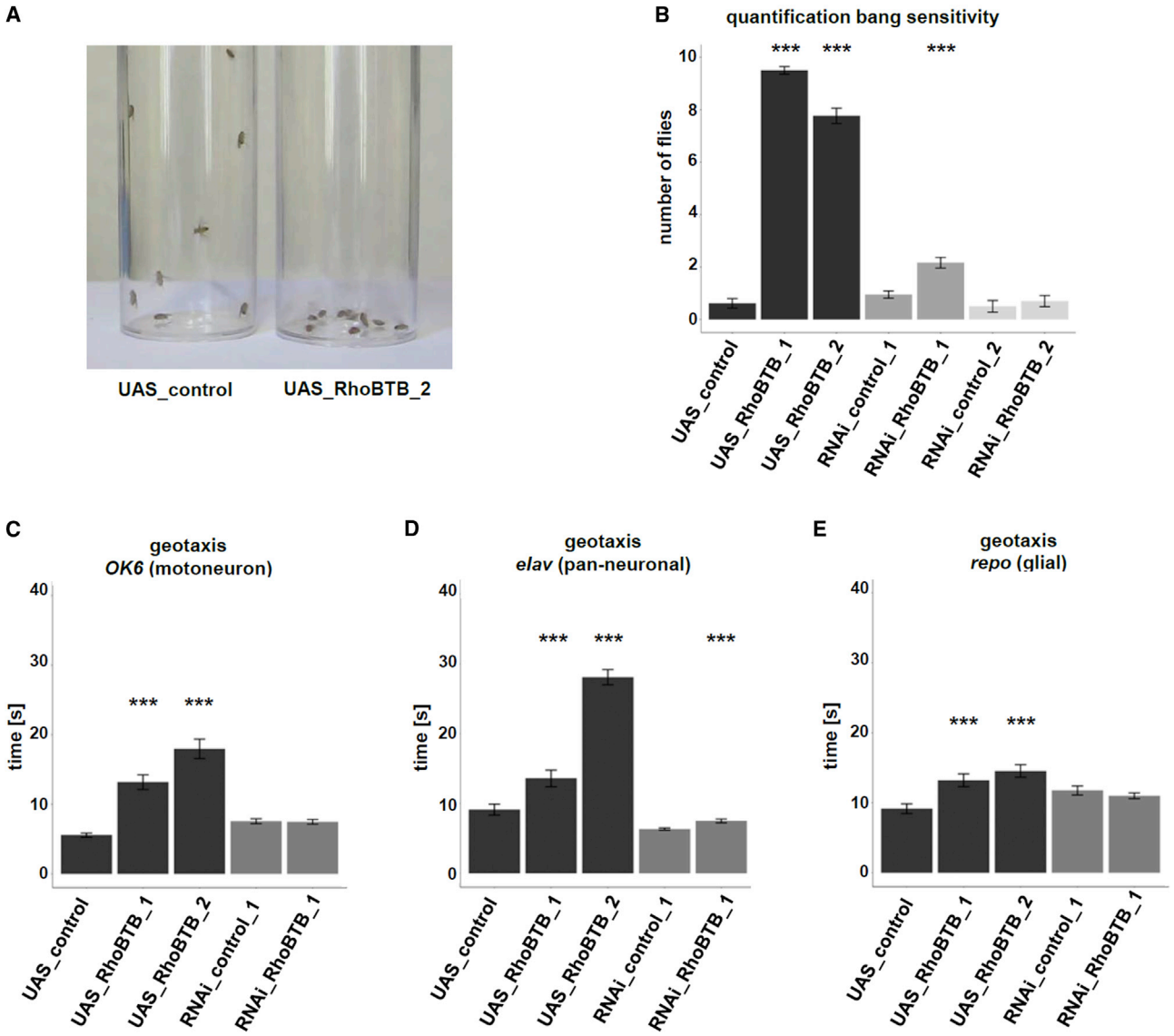

Figure 3. The Impact of Altered Amounts of RhoBTB on Fruit Fly Behavior

(A) Flies overexpressing *RhoBTB* pan-neuronally (UAS_RhoBTB_2) showed bang-sensitivity phenotypes after vortexing. All ten flies, paralyzed and with spasms, were at the bottom of the vial, whereas flies from the corresponding genetic background line already started to walk up the sides (see also Movie S1).

(B) Quantification of the number of flies (either overexpressing *RhoBTB* or upon knockdown) shaking on the bottom of the vial 5 s after vortexing. The diagram shows the mean value from a minimum number of 100 flies tested per genotype ± SEM.

(C–E) Flies overexpressing *RhoBTB* in motoneurons (C), in all neurons (D), or in glia (E) (black bars) showed significant locomotor impairment in the negative geotaxis assay, as measured by the amount of time that 70% of flies in a vial needed to crawl up 8.8 cm after being tapped down. Only knockdown in all neurons (D), but not in motoneurons or glia (C and E; gray bars), resulted in significant locomotor impairment. Data represent the mean from a minimum of 300 flies tested per genotype ± SEM. Asterisks indicate statistical significance (**$p < 0.01$, ***$p < 0.001$).

Altered Dosage of RhoBTB in *Drosophila* Has No Impact on Synapse Morphology but Leads to Impaired Dendrite Development

On the basis of the severe locomotor phenotype, we investigated whether there was a correlate in terms of altered development and morphology of NMJs (Figure 4A). Overexpression of *RhoBTB* in motoneurons with the *OK6*-GAL4 promoter did not result in any significant alterations of NMJ morphology (Figure 4B), and neither did overexpression using the *D42*-GAL4 or a pan-neuronal driver (Figure S11A and S11B). Also, knockdown of *RhoBTB* in motoneurons or pan-neuronally did not reveal consistent differences from the respective controls (Figures S11C–S11G).

Drosophila class IV da neurons are a good model for studying dendritic morphology.[38] Knockdown of *RhoBTB* in these neurons with a combination of the *477*-GAL4 and *pkk*-GAL4 drivers[21] resulted in a significantly reduced number of dendritic branches in the medially located da neurons for both tested RNAi lines, as well as a markedly

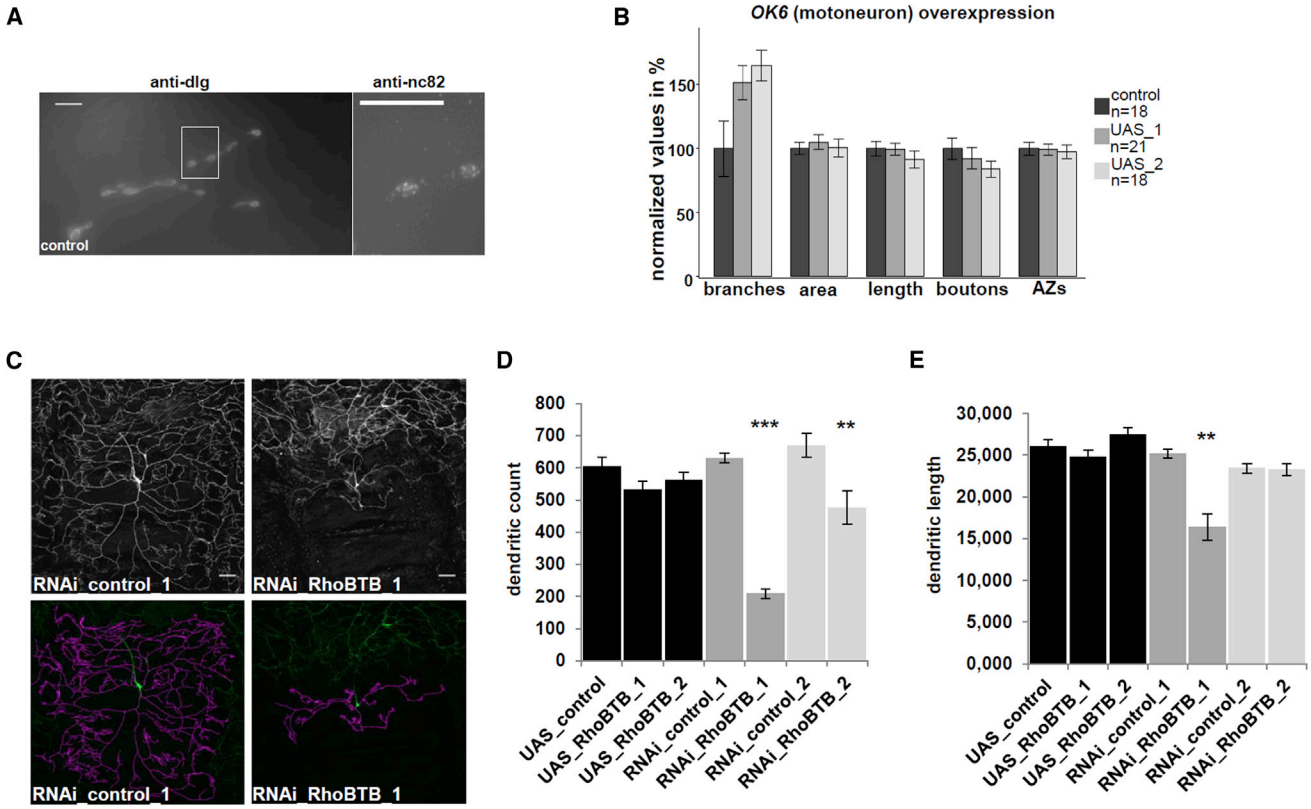

Figure 4. The Impact of Altered Amounts of RhoBTB on Fly Synaptic and Dendritic Morphology
(A) Representative pictures of a NMJ from a control larva. The white-framed box indicates the cutout on the right side. NMJ area and length and the number of synaptic boutons were determined from staining with anti-dlg (post-synaptic protein discs large), and the number of active zones was determined from staining with anti-nc82 (pre-synaptic protein bruchpilot). Scale bars represent 10 μm.
(B) Quantification did not reveal significant alterations in NMJ morphology upon *RhoBTB* overexpression using the *OK6*-GAL4 motoneuron driver.
(C) Representative class IV da neurons showing smaller size and abnormal dendritic morphology upon knockdown of *RhoBTB* in comparison with control larvae. In the lower panel, tracing of dendritic branches with NeuronJ is displayed. Scale bars represent 50 μm.
(D and E) Quantification of ten da neurons from three to five different animals per genotype. They showed no alteration upon overexpression but did show a significantly reduced number (D) and/or mean length (E) of dendritic branches upon knockdown. Error bars represent the SEM. Asterisks indicate statistical significance (**$p < 0.01$, ***$p < 0.001$). AZ stands for active zone.

reduced total size and length of dendritic branches for one of the lines (RNAi_RhoBTB_1). Differences in severity of the phenotype between the two lines might be due to a slightly stronger knockdown effect for RNAi_RhoBTB_1 (Figure S2). Overexpression did not result in significant changes in the evaluated parameters (Figures 4C–4E).

Discussion

De Novo Missense Variants in *RHOBTB2* Cause a Developmental and Epileptic Encephalopathy

We identified *de novo* missense variants in *RHOBTB2* in ten individuals with a developmental and epileptic encephalopathy. Their highly similar phenotype includes early-onset seizures, severe to profound ID, postnatal microcephaly, and movement disorders. It considerably overlaps other early-onset epileptic disorders with acquired microcephaly and movement anomalies, such as CDKL5-, FOXG1-, or SLC2A1- related encephalopathies (early infantile epileptic encephalopathy 2 [MIM: 300672], Rett syndrome [MIM: 613454], and GLUT1 deficiency syndrome 1 [MIM: 606777]), many of which were previously excluded in the individuals in our study. Therefore, diagnosis of *RHOBTB2*-related developmental and epileptic encephalopathy might rely on panel or exome sequencing rather than on a specific clinical suspicion. Aspects that might be more specifically related to *RHOBTB2* are (post-ictal) hemiparesis (observed in four individuals) and secondary MRI anomalies (described in three of the four). This needs follow-up in further studies because it might be relevant to prognosis. The reported regression in several individuals and the correlation between relatively mild or late-onset epilepsy in individuals 8 and 10 and a milder psychomotor and neurological impairment might indicate that *RHOBTB2* aberrations result in severe cognitive impairment secondary to or contributed to by seizures.

Rho-related BTB-domain-containing proteins constitute a subfamily of atypical Rho GTPases, represented in mammals by RHOBTB1, RHOBTB2, and RHOBTB3. Of the three

encoding genes, *RHOBTB2* seems to be most abundantly expressed in the nervous system.[35] Very distinct among all small GTPases is their domain architecture, which consists of the Rho GTPase region immediately followed by a short proline-rich region, a tandem of two BTB domains, and a C-terminal region.[39] In contrast to typical Rho GTPases, no specific guanine nucleotide exchange factors or GTPase-activating proteins are known to activate atypical Rho GTPases. Instead, an activating mechanism that relieves its auto-inhibited conformation through interaction with other proteins and an inactivating mechanism that acts through auto-ubiquitination and degradation in the proteasome have been discussed.[40] The BTB domains allow formation of homodimers and heterodimers with other proteins of the RhoBTB subfamily. They also bind to their own GTPase domain and to the ubiquitin ligase scaffold CUL3.[33] The latter interaction mediates auto-ubiquitination and thus inactivation of RHOBTB2 by the cullin-3-dependent ubiquitin ligase complex, followed by proteasomal degradation.[33,34,41]

After the initial observation that *RHOBTB2* (also called *DBC2*) was homozygously deleted in breast cancer,[42] mainly a role in tumorigenesis and as a possible tumor suppressor has been reported.[40] The only indication that *RHOBTB2*, in accordance with its high expression in neuronal tissues,[35,43] might be involved in neurodevelopmental disorders came from the report of a single individual affected by a Rett-syndrome-like phenotype including epilepsy and a lack of speech and carrying a *de novo* missense variant (c.1528A>G [p.Asn510Asp]) in *RHOBTB2* in addition to a *de novo* missense variant (c.602G>A [p.Arg201His]) in *EIF4G1* (MIM: 600495).[31]

This published variant and all variants identified in our cohort cluster within the first BTB domain (Ala474 and Arg483) or at the dimer interface of the second BTB domain (Asn510 and Arg511), and two arginines at positions 483 and 511 and an asparagine at position 510 are recurrently affected. This is in accordance with a recent study demonstrating that pathogenic missense variants often cluster in hotspots and domains.[44] Of note, individual 10, the only one with an affected alanine at position 474, has a milder phenotype including febrile seizures only, a walking age of 18 months, speech limited to a few words and two-word combinations, and a lack of abnormal movements. This might point to a genotype-phenotype correlation that has to be further delineated in future studies. The apparent rarity of *RHOBTB2*-associated developmental and epileptic encephalopathy prevented the identification of a sufficient number of variants to reach significance in large-scale studies, such as the Deciphering Developmental Disorders Study, in which only one *de novo* variant in *RHOBTB2* was identified in 4,293 individuals with severe developmental disorders.[6] However, contacting colleagues and searching databases such as DECIPHER[7] and exchanging platforms such as GeneMatcher[8] were powerful tools for assembling a critical number of variants and individuals. With ten individuals displaying a highly similar phenotype, the *de novo* occurrence and clustering of variants, pathogenic prediction, and functional tests, we provide all currently possible lines of evidence for the pathogenicity of the identified variants in *RHOBTB2*.

Given the constraint scores from the ExAC Browser and the fact that the *de novo* variants identified here cluster within and between the BTB domains, altered protein function by a specific domain-related effect is more likely than haploinsufficiency or LoF. Previous, cancer-related studies on *RHOBTB2* have suggested impaired binding of mutant RHOBTB2 to CUL3 and therefore to the cullin-3-dependent ubiquitin ligase complex, which results in reduced ubiquitination and degradation of both RHOBTB2 itself and possibly other substrates via the proteasome.[33,41] Variants in a specific splice site of *CUL3* (MIM: 603136) are implicated in pseudohypoaldosteronism type II E (MIM: 614496), and interestingly, several *de novo* variants in *CUL3* have been reported in individuals with developmental delay or ASD.[6,45–47] By co-immunoprecipitation, we could not observe impaired binding between CUL3 and RHOBTB2 carrying one of three different variants. This finding is in line with the structural data from homologous CUL3-BTB complexes, indicating that the cullin-3 binding site is located in the second BTB domain[15] but is distant from the site of the p.Asn510Asp, p.Arg511Gln, and p.Arg511Trp variants. Thus, neither these variants nor p.Ala474Gly or p.Arg483His, located in the first BTB domain, is expected to disrupt the CUL3 binding site of RHOBTB2. However, findings of more mutant than wild-type RHOBTB2 in transfected cells without proteasome inhibitor and equal amounts in cells treated with proteasome inhibitor indicate that the variants still might have an effect on proper ubiquitination and degradation of RHOBTB2 in the proteasome. This is probably not mediated by a direct interaction with CUL3 but rather by impaired BTB-domain stability or dimer formation. Increased amounts of RHOBTB2 and other RHOBTB2-dependent substrates might therefore be relevant to the phenotype, although increased amounts could not be tested in material from affected individuals, and (additional) dominant-negative or neomorphic effects of the variants cannot be excluded. Mutations in several components of the ubiquitin-proteasome system have been reported in ID disorders, e.g., defects in ubiquitin ligase *UBE3A* (MIM: 601623) in Angelman syndrome (MIM: 105830) or, more recently, mutations in the proteasome regulatory subunit *PSMD12* (MIM: 604450) in Stankiewitz-Isidor syndrome (MIM: 617516).

Altered Dosage of *RhoBTB* in *Drosophila* Results in Seizure Susceptibility and Other Neurological Phenotypes

So far, mainly the role of somatic deletions or mutations of *RHOBTB2* in various cancers and tumorigenesis has been investigated and discussed.[42,48–50] *RHOBTB2* now joins the growing list of genes implicated in both cancer and developmental disorders.[51] To confirm and further

characterize the role of RHOBTB2 for cognitive and neurological phenotypes, we chose *Drosophila melanogaster* as a model organism because it has demonstrated its great value for such objectives.[27,52,53] Given that the identified variants in *RHOBTB2* seem to result in impaired degradation and thus increased amounts of protein, manipulating the amount of RhoBTB in the fruit fly by tissue-specific knockdown and particularly overexpression appeared to be a very suitable approach. In accordance with the human phenotype, we found seizure susceptibility that was more severe upon pan-neuronal overexpression than upon knockdown. However, it has to be considered that elevated amounts of *Drosophila* RhoBTB due to very strong overexpression might have been considerably higher than those in cell culture or possibly in tissues from affected individuals. Severe, gross neurological and locomotor defects were observed upon overexpression of *RhoBTB* in all neurons and particularly in motoneurons, whereas complex learning and memory processes were unaffected. This might possibly support a contributory effect of epileptic activity to the severity of ID in affected human individuals. Interestingly, we also observed a geotaxis phenotype upon overexpression of *RhoBTB* in fly glial cells, indicating a broader role of RhoBTB in the nervous system. The observation of more severe neurological phenotypes upon overexpression of *RhoBTB* than upon knockdown is in line with the assumption that increased amounts of RHOBTB2 rather than haploinsufficiency or LoF is the disease-causing mechanism in humans.

On the basis of the observed severe locomotor defects upon overexpression of RhoBTB, we wondered whether this was accompanied by a morphological correlate in neuromuscular synapses. Fly NMJs are giant synapses that share a series of features with central excitatory synapses in the mammalian brain and represent an established model for the study of synaptic development and plasticity.[54] However, we found no consistent NMJ phenotype after the amount of RhoBTB was altered. The severe locomotor defects we observed are therefore probably not solely related to developmental or morphological NMJ alterations. There could be an underlying functional defect, e.g., in neurotransmitter transport, that would not be detected by our assay. A role of RHOBTB2 in vesicle trafficking, but not within synapses, has previously been discussed.[40] Alternatively, tapping down flies in the negative geotaxis assay might already provoke a mild manifestation of bang sensitivity and thus impair locomotor behavior.

Typical Rho GTPases are known to be key regulators of the actin and microtubule cytoskeleton by playing roles in dendrite and dendritic spine development and morphology.[55] For several Rho-linked ID-associated proteins, a role in spine morphogenesis has been demonstrated.[56,57] For atypical Rho GTPases, such functions are not yet characterized, and specifically for RHOBTB2, only a minor role in the organization of the actin cytoskeleton has been discussed so far.[58] Using *Drosophila*, we have now demonstrated a possible contribution of RhoBTB to proper dendrite organization given that knockdown of *RhoBTB* in da neurons resulted in a significantly reduced number of dendritic branches.

In summary, we have identified *de novo* missense variants in *RHOBTB2* as a cause of developmental and epileptic encephalopathy. We observed an increased amount of mutant RHOBTB2 and could demonstrate a crucial role of its *Drosophila* ortholog, RhoBTB, in seizure susceptibility, neurological function, and dendrite development.

Accession Numbers

The accession numbers for the variants reported in this paper are LOVD: 00133649–00133659.

Supplemental Data

Supplemental Data include 11 figures, 1 table, and 1 movie and can be found with this article online at https://doi.org/10.1016/j.ajhg.2017.11.008.

Conflicts of Interest

Z.P. is an employee of Ambry Genetics.

Acknowledgments

We thank all affected individuals and their families for participating in this study. We thank Laila Distel, Christine Suchy, and Nicole Rachinger for excellent technical assistance; Jessica Panzer for providing clinical details; and Annette Schenck, Monique van der Voet, and Tom Koemans for providing fly lines and helping with the courtship conditioning assay. We also thank André Reis (supported by German Ministry of Education and Research 01GS08160), Arif Ekici, and Steffen Uebe from the next-generation sequencing core facility at the Institute of Human Genetics in Erlangen. We thank Felix Engel and Silvia Vergarajauregui for helping with confocal microscopy, which was supported by the German Research Foundation (INST 410/91-1 FUGG). This study made use of data generated by the DECIPHER community. A full list of centers that contributed to the generation of the data is available at http://decipher.sanger.ac.uk and via email at decipher@sanger.ac.uk. Funding for the project was provided by the Wellcome Trust. Fly stocks were obtained from the Bloomington *Drosophila* Stock Center (NIH P40OD018537), the *Drosophila* Transgenic RNAi Project at Harvard Medical School (NIH National Institute of General Medical Sciences R01-GM084947), and the Vienna *Drosophila* Resource Center (http://www.vdrc.at). Antibodies from the Developmental Studies Hybridoma Bank (created by the NIH National Institute of Child Health and Human Development) were used in this study. X.O.G. is supported by the Harold Amos Faculty Development Award of the Robert Wood Johnson Foundation, A.P. is supported by the Boston Children's Hospital Translational Research Program, and C.Z. is supported by grants from the German Research Foundation (ZW184/1-2, ZW184/3-1, and GRK2162) and by the Interdisciplinary Center for Clinical Research in Erlangen (E26).

Received: August 22, 2017
Accepted: November 16, 2017
Published: December 21, 2017

Web Resources

Clustal Omega, http://www.ebi.ac.uk/Tools/msa/clustalo/
ExAC Browser, http://exac.broadinstitute.org/
GenBank, https://www.ncbi.nlm.nih.gov/genbank/
GnomAD, http://gnomad.broadinstitute.org/
Homologene, https://www.ncbi.nlm.nih.gov/homologene
LOVD, http://www.lovd.nl/3.0/home
OMIM, http://www.omim.org/
Primer X, http://www.bioinformatics.org/primerx/
SMART, http://smart.embl-heidelberg.de/
SysID, http://sysid.cmbi.umcn.nl/
Treefam, http://www.treefam.org/
UCSC Genome Browser, http://genome.ucsc.edu/

References

1. Kochinke, K., Zweier, C., Nijhof, B., Fenckova, M., Cizek, P., Honti, F., Keerthikumar, S., Oortveld, M.A., Kleefstra, T., Kramer, J.M., et al. (2016). Systematic Phenomics Analysis Deconvolutes Genes Mutated in Intellectual Disability into Biologically Coherent Modules. Am. J. Hum. Genet. *98*, 149–164.
2. de Ligt, J., Willemsen, M.H., van Bon, B.W., Kleefstra, T., Yntema, H.G., Kroes, T., Vulto-van Silfhout, A.T., Koolen, D.A., de Vries, P., Gilissen, C., et al. (2012). Diagnostic exome sequencing in persons with severe intellectual disability. N. Engl. J. Med. *367*, 1921–1929.
3. Rauch, A., Wieczorek, D., Graf, E., Wieland, T., Endele, S., Schwarzmayr, T., Albrecht, B., Bartholdi, D., Beygo, J., Di Donato, N., et al. (2012). Range of genetic mutations associated with severe non-syndromic sporadic intellectual disability: an exome sequencing study. Lancet *380*, 1674–1682.
4. Vissers, L.E., de Ligt, J., Gilissen, C., Janssen, I., Steehouwer, M., de Vries, P., van Lier, B., Arts, P., Wieskamp, N., del Rosario, M., et al. (2010). A de novo paradigm for mental retardation. Nat. Genet. *42*, 1109–1112.
5. O'Roak, B.J., Deriziotis, P., Lee, C., Vives, L., Schwartz, J.J., Girirajan, S., Karakoc, E., Mackenzie, A.P., Ng, S.B., Baker, C., et al. (2011). Exome sequencing in sporadic autism spectrum disorders identifies severe de novo mutations. Nat. Genet. *43*, 585–589.
6. Deciphering Developmental Disorders Study (2017). Prevalence and architecture of de novo mutations in developmental disorders. Nature *542*, 433–438.
7. Firth, H.V., Richards, S.M., Bevan, A.P., Clayton, S., Corpas, M., Rajan, D., Van Vooren, S., Moreau, Y., Pettett, R.M., and Carter, N.P. (2009). DECIPHER: Database of Chromosomal Imbalance and Phenotype in Humans Using Ensembl Resources. Am. J. Hum. Genet. *84*, 524–533.
8. Sobreira, N., Schiettecatte, F., Valle, D., and Hamosh, A. (2015). GeneMatcher: a matching tool for connecting investigators with an interest in the same gene. Hum. Mutat. *36*, 928–930.
9. Kumar, P., Henikoff, S., and Ng, P.C. (2009). Predicting the effects of coding non-synonymous variants on protein function using the SIFT algorithm. Nat. Protoc. *4*, 1073–1081.
10. Adzhubei, I.A., Schmidt, S., Peshkin, L., Ramensky, V.E., Gerasimova, A., Bork, P., Kondrashov, A.S., and Sunyaev, S.R. (2010). A method and server for predicting damaging missense mutations. Nat. Methods *7*, 248–249.
11. Schwarz, J.M., Cooper, D.N., Schuelke, M., and Seelow, D. (2014). MutationTaster2: mutation prediction for the deep-sequencing age. Nat. Methods *11*, 361–362.
12. Jagadeesh, K.A., Wenger, A.M., Berger, M.J., Guturu, H., Stenson, P.D., Cooper, D.N., Bernstein, J.A., and Bejerano, G. (2016). M-CAP eliminates a majority of variants of uncertain significance in clinical exomes at high sensitivity. Nat. Genet. *48*, 1581–1586.
13. Wu, S., and Zhang, Y. (2007). LOMETS: a local meta-threading-server for protein structure prediction. Nucleic Acids Res. *35*, 3375–3382.
14. Ahmad, K.F., Melnick, A., Lax, S., Bouchard, D., Liu, J., Kiang, C.L., Mayer, S., Takahashi, S., Licht, J.D., and Privé, G.G. (2003). Mechanism of SMRT corepressor recruitment by the BCL6 BTB domain. Mol. Cell *12*, 1551–1564.
15. Canning, P., Cooper, C.D., Krojer, T., Murray, J.W., Pike, A.C., Chaikuad, A., Keates, T., Thangaratnarajah, C., Hojzan, V., Ayinampudi, V., et al. (2013). Structural basis for Cul3 protein assembly with the BTB-Kelch family of E3 ubiquitin ligases. J. Biol. Chem. *288*, 7803–7814.
16. Guex, N., and Peitsch, M.C. (1997). SWISS-MODEL and the Swiss-PdbViewer: an environment for comparative protein modeling. Electrophoresis *18*, 2714–2723.
17. Sayle, R.A., and Milner-White, E.J. (1995). RASMOL: biomolecular graphics for all. Trends Biochem. Sci. *20*, 374.
18. Schneider, C.A., Rasband, W.S., and Eliceiri, K.W. (2012). NIH Image to ImageJ: 25 years of image analysis. Nat. Methods *9*, 671–675.
19. Brand, A.H., and Perrimon, N. (1993). Targeted gene expression as a means of altering cell fates and generating dominant phenotypes. Development *118*, 401–415.
20. Ni, J.Q., Liu, L.P., Binari, R., Hardy, R., Shim, H.S., Cavallaro, A., Booker, M., Pfeiffer, B.D., Markstein, M., Wang, H., et al. (2009). A Drosophila resource of transgenic RNAi lines for neurogenetics. Genetics *182*, 1089–1100.
21. Zazo Seco, C., Castells-Nobau, A., Joo, S.H., Schraders, M., Foo, J.N., van der Voet, M., Velan, S.S., Nijhof, B., Oostrik, J., de Vrieze, E., et al. (2017). A homozygous FITM2 mutation causes a deafness-dystonia syndrome with motor regression and signs of ichthyosis and sensory neuropathy. Dis. Model. Mech. *10*, 105–118.
22. Perkins, L.A., Holderbaum, L., Tao, R., Hu, Y., Sopko, R., McCall, K., Yang-Zhou, D., Flockhart, I., Binari, R., Shim, H.S., et al. (2015). The Transgenic RNAi Project at Harvard Medical School: Resources and Validation. Genetics *201*, 843–852.
23. Dietzl, G., Chen, D., Schnorrer, F., Su, K.C., Barinova, Y., Fellner, M., Gasser, B., Kinsey, K., Oppel, S., Scheiblauer, S., et al. (2007). A genome-wide transgenic RNAi library for conditional gene inactivation in Drosophila. Nature *448*, 151–156.
24. Green, E.W., Fedele, G., Giorgini, F., and Kyriacou, C.P. (2014). A Drosophila RNAi collection is subject to dominant phenotypic effects. Nat. Methods *11*, 222–223.
25. Kuebler, D., and Tanouye, M.A. (2000). Modifications of seizure susceptibility in Drosophila. J. Neurophysiol. *83*, 998–1009.
26. Palladino, M.J., Hadley, T.J., and Ganetzky, B. (2002). Temperature-sensitive paralytic mutants are enriched for those causing neurodegeneration in Drosophila. Genetics *161*, 1197–1208.
27. Gregor, A., Kramer, J.M., van der Voet, M., Schanze, I., Uebe, S., Donders, R., Reis, A., Schenck, A., and Zweier, C. (2014).

Altered GPM6A/M6 dosage impairs cognition and causes phenotypes responsive to cholesterol in human and Drosophila. Hum. Mutat. *35*, 1495–1505.
28. Grueber, W.B., Jan, L.Y., and Jan, Y.N. (2002). Tiling of the Drosophila epidermis by multidendritic sensory neurons. Development *129*, 2867–2878.
29. Meijering, E., Jacob, M., Sarria, J.C., Steiner, P., Hirling, H., and Unser, M. (2004). Design and validation of a tool for neurite tracing and analysis in fluorescence microscopy images. Cytometry A *58*, 167–176.
30. Schultz, J., Milpetz, F., Bork, P., and Ponting, C.P. (1998). SMART, a simple modular architecture research tool: identification of signaling domains. Proc. Natl. Acad. Sci. USA *95*, 5857–5864.
31. Lopes, F., Barbosa, M., Ameur, A., Soares, G., de Sá, J., Dias, A.I., Oliveira, G., Cabral, P., Temudo, T., Calado, E., et al. (2016). Identification of novel genetic causes of Rett syndrome-like phenotypes. J. Med. Genet. *53*, 190–199.
32. Lek, M., Karczewski, K.J., Minikel, E.V., Samocha, K.E., Banks, E., Fennell, T., O'Donnell-Luria, A.H., Ware, J.S., Hill, A.J., Cummings, B.B., et al.; Exome Aggregation Consortium (2016). Analysis of protein-coding genetic variation in 60,706 humans. Nature *536*, 285–291.
33. Berthold, J., Schenková, K., Ramos, S., Miura, Y., Furukawa, M., Aspenström, P., and Rivero, F. (2008). Characterization of RhoBTB-dependent Cul3 ubiquitin ligase complexes–evidence for an autoregulatory mechanism. Exp. Cell Res. *314*, 3453–3465.
34. Wilkins, A., and Carpenter, C.L. (2008). Regulation of RhoBTB2 by the Cul3 ubiquitin ligase complex. Methods Enzymol. *439*, 103–109.
35. Ramos, S., Khademi, F., Somesh, B.P., and Rivero, F. (2002). Genomic organization and expression profile of the small GTPases of the RhoBTB family in human and mouse. Gene *298*, 147–157.
36. Pavlidis, P., and Tanouye, M.A. (1995). Seizures and failures in the giant fiber pathway of Drosophila bang-sensitive paralytic mutants. J. Neurosci. *15*, 5810–5819.
37. Zars, T. (2000). Behavioral functions of the insect mushroom bodies. Curr. Opin. Neurobiol. *10*, 790–795.
38. Jan, Y.N., and Jan, L.Y. (2010). Branching out: mechanisms of dendritic arborization. Nat. Rev. Neurosci. *11*, 316–328.
39. Aspenström, P., Ruusala, A., and Pacholsky, D. (2007). Taking Rho GTPases to the next level: the cellular functions of atypical Rho GTPases. Exp. Cell Res. *313*, 3673–3679.
40. Ji, W., and Rivero, F. (2016). Atypical Rho GTPases of the RhoBTB Subfamily: Roles in Vesicle Trafficking and Tumorigenesis. Cells *5*. https://doi.org/10.3390/cells5020028.
41. Wilkins, A., Ping, Q., and Carpenter, C.L. (2004). RhoBTB2 is a substrate of the mammalian Cul3 ubiquitin ligase complex. Genes Dev. *18*, 856–861.
42. Hamaguchi, M., Meth, J.L., von Klitzing, C., Wei, W., Esposito, D., Rodgers, L., Walsh, T., Welcsh, P., King, M.C., and Wigler, M.H. (2002). DBC2, a candidate for a tumor suppressor gene involved in breast cancer. Proc. Natl. Acad. Sci. USA *99*, 13647–13652.
43. St-Pierre, B., Jiang, Z., Egan, S.E., and Zacksenhaus, E. (2004). High expression during neurogenesis but not mammogenesis of a murine homologue of the Deleted in Breast Cancer2/Rhobtb2 tumor suppressor. Gene Expr. Patterns *5*, 245–251.
44. Geisheker, M.R., Heymann, G., Wang, T., Coe, B.P., Turner, T.N., Stessman, H.A.F., Hoekzema, K., Kvarnung, M., Shaw, M., Friend, K., et al. (2017). Hotspots of missense mutation identify neurodevelopmental disorder genes and functional domains. Nat. Neurosci. *20*, 1043–1051.
45. Codina-Solà, M., Rodríguez-Santiago, B., Homs, A., Santoyo, J., Rigau, M., Aznar-Laín, G., Del Campo, M., Gener, B., Gabau, E., Botella, M.P., et al. (2015). Integrated analysis of whole-exome sequencing and transcriptome profiling in males with autism spectrum disorders. Mol. Autism *6*, 21.
46. Stessman, H.A., Xiong, B., Coe, B.P., Wang, T., Hoekzema, K., Fenckova, M., Kvarnung, M., Gerdts, J., Trinh, S., Cosemans, N., et al. (2017). Targeted sequencing identifies 91 neurodevelopmental-disorder risk genes with autism and developmental-disability biases. Nat. Genet. *49*, 515–526.
47. Wang, T., Guo, H., Xiong, B., Stessman, H.A., Wu, H., Coe, B.P., Turner, T.N., Liu, Y., Zhao, W., Hoekzema, K., et al. (2016). De novo genic mutations among a Chinese autism spectrum disorder cohort. Nat. Commun. *7*, 13316.
48. Cho, Y.G., Choi, B.J., Kim, C.J., Song, J.H., Zhang, C., Nam, S.W., Lee, J.Y., and Park, W.S. (2008). Genetic analysis of the DBC2 gene in gastric cancer. Acta Oncol. *47*, 366–371.
49. Knowles, M.A., Aveyard, J.S., Taylor, C.F., Harnden, P., and Bass, S. (2005). Mutation analysis of the 8p candidate tumour suppressor genes DBC2 (RHOBTB2) and LZTS1 in bladder cancer. Cancer Lett. *225*, 121–130.
50. Ohadi, M., Totonchi, M., Maguire, P., Lindblom, A., Habibi, R., Alavi, B.A., Keyhani, E., and Najmabadi, H. (2007). Mutation analysis of the DBC2 gene in sporadic and familial breast cancer. Acta Oncol. *46*, 770–772.
51. Crawley, J.N., Heyer, W.D., and LaSalle, J.M. (2016). Autism and Cancer Share Risk Genes, Pathways, and Drug Targets. Trends Genet. *32*, 139–146.
52. Kramer, J.M., Kochinke, K., Oortveld, M.A., Marks, H., Kramer, D., de Jong, E.K., Asztalos, Z., Westwood, J.T., Stunnenberg, H.G., Sokolowski, M.B., et al. (2011). Epigenetic regulation of learning and memory by Drosophila EHMT/G9a. PLoS Biol. *9*, e1000569.
53. Zweier, C., de Jong, E.K., Zweier, M., Orrico, A., Ousager, L.B., Collins, A.L., Bijlsma, E.K., Oortveld, M.A., Ekici, A.B., Reis, A., et al. (2009). CNTNAP2 and NRXN1 are mutated in autosomal-recessive Pitt-Hopkins-like mental retardation and determine the level of a common synaptic protein in Drosophila. Am. J. Hum. Genet. *85*, 655–666.
54. Koh, Y.H., Gramates, L.S., and Budnik, V. (2000). Drosophila larval neuromuscular junction: molecular components and mechanisms underlying synaptic plasticity. Microsc. Res. Tech. *49*, 14–25.
55. Ba, W., van der Raadt, J., and Nadif Kasri, N. (2013). Rho GTPase signaling at the synapse: implications for intellectual disability. Exp. Cell Res. *319*, 2368–2374.
56. Govek, E.E., Newey, S.E., Akerman, C.J., Cross, J.R., Van der Veken, L., and Van Aelst, L. (2004). The X-linked mental retardation protein oligophrenin-1 is required for dendritic spine morphogenesis. Nat. Neurosci. *7*, 364–372.
57. Nodé-Langlois, R., Muller, D., and Boda, B. (2006). Sequential implication of the mental retardation proteins ARHGEF6 and PAK3 in spine morphogenesis. J. Cell Sci. *119*, 4986–4993.
58. Aspenström, P., Fransson, A., and Saras, J. (2004). Rho GTPases have diverse effects on the organization of the actin filament system. Biochem. J. *377*, 327–337.